JOURNAL OF GEOPHYSICAL RESEARCH, VOL. 86, NO. B4, PAGES 3039–3054, APRIL 10, 1981

Bidirectional Reflectance Spectroscopy 1. Theory

BRUCE HAPKE

Department of Geology and Planetary Science, University of Pittsburgh, Pittsburgh, Pennsylvania 15260

An approximate analytic solution to the radiative transfer equation describing the scattering of light from particulate surfaces is derived. Multiple scattering and mutual shadowing are taken into account. Analytic expressions for the following quantities are found: bidirectional reflectance, radiance factor, radiance coefficient, normal, hemispherical, Bond, and physical albedos, integral phase function, phase integral, and limb-darkening profile. Scattering functions for mixtures can be calculated, as well as corrections for comparing experimental laboratory transmission or reflection spectra with observational planetary spectra. An expression for the scattering efficiency of an irregular particle large compared with the wavelength is derived. For closely spaced, nonopaque particles this efficiency is approximated by $(1 + \alpha D_e)^{-1}$, where α is the true absorption coefficient and D_e is an effective particle diameter of the order of twice the mean particle size. For monomineralic surfaces it is shown that $\alpha = (1 - w)/wD_e$, where w is the single-scattering albedo and can be determined from reflectance measurements of a powder, so that α may be calculated from reflectance. This theory should be useful for interpretations of reflectance spectroscopy of laboratory surfaces and photometry of solar system objects. From photometric observations of a body the following may be estimated: average single-scattering albedo, average particle phase function, average macroscopic slope, and porosity.

1. INTRODUCTION

In this paper a number of expressions related to the diffuse scattering of light from the surface of a semi-infinite particle medium are derived. Observational and laboratory data which support this theory are presented in a companion paper [*Hapke and Wells,* this issue], hereafter referred to as paper II. These expressions should be useful for first-order interpretations of photometry and spectroscopy of planetary surfaces and clouds and of laboratory particulate surfaces. The general philosophy of this paper will be to derive analytic expressions which, although admittedly approximate, nevertheless describe the essential physics of the scattering process and have errors within the accuracy with which absolute planetary reflectances can be measured, about ±10%.

Such a theory is of interest for several reasons. First, although the theoretical basis for scattering of light from dispersed particulate media is well established [e.g., *Chandrasekhar,* 1960; *Irvine,* 1975; *Van de Hulst,* 1963; *Hansen and Travis,* 1974], no general theory exists for a surface in which the particles are close together. Present theories for such surfaces are either empirical, such as the generalized Lambert or Minnaert law [*Minnaert,* 1941] or the *Meador and Weaver* [1975] expression, or require extensive computer calculations. The theory presented here is solidly based on the equation of radiative transfer but is sufficiently simple that programable hand calculators can be used for numerical evaluation.

Second, the bidirectional reflectance is usually the quantity measured when carrying out photometry or spectroscopy of planetary surfaces. It may then be compared with laboratory measurements on candidate materials. The laboratory data may be transmittance or bidirectional or directional-hemispherical reflectance, and the materials are of different particle size and state of compaction than the planetary surface. A method of correcting one data set for direct comparison with the other is of obvious interest.

Third, in most planetary applications one is interested in an inversion of the scattering problem. That is, from the measured scattering properties of the surface one wishes to determine the more fundamental physical properties, such as absorption coefficient. Because in planetary applications the absolute accuracy is not high, exact numerical solutions are no more useful, and much less convenient, than approximate analytic ones.

This rest of the paper is divided into three major parts. In the section 2 the bidirectional reflectance function is obtained for a medium of dispersed particles of arbitrary single-scattering albedo and phase function. The changes which occur in the scattering law when the particles are brought close together, as in a planetary surface regolith, are discussed. In section 3, scattering from a single irregular particle of the medium is considered. A useful approximate relation between scattering efficiency and true absorption coefficient is deduced. Section 4 discusses applications to planetary and laboratory problems. Expressions for several types of albedos and reflectances encountered in planetary photometry are derived.

The notation used in this paper is listed for convenience in the notation section. Wherever possible, the nomenclature used here is that recommended by *Nicodemus* [1965] and *Judd* [1967].

2. THE BIDIRECTIONAL REFLECTANCE FUNCTION

a. *Solution of the Radiative Transfer Equation for Dispersed Particles*

Consider a plane surface at $z = 0$ which separates an empty half space $z > 0$ from a half space $z < 0$ containing irregular, randomly oriented, absorbing particles which are large compared with the wavelength. Initially, it will be assumed that the particles are so far apart on the average that shadowing of one particle by another is negligible. This requirement will be relaxed in the next section. Reflectances of planetary regoliths or cloud tops are of interest in this paper. Thus it is assumed that the medium in which the particles are imbedded has an index of refraction equal to unity and that no physical surface separates the two half spaces. The medium is illuminated by collimated light of intensity J traveling into a direction which makes an angle $(\pi - i)$ with the upward z-direction and has an

Paper number 80B1488.
0148-0227/81/080B-1488$01.00

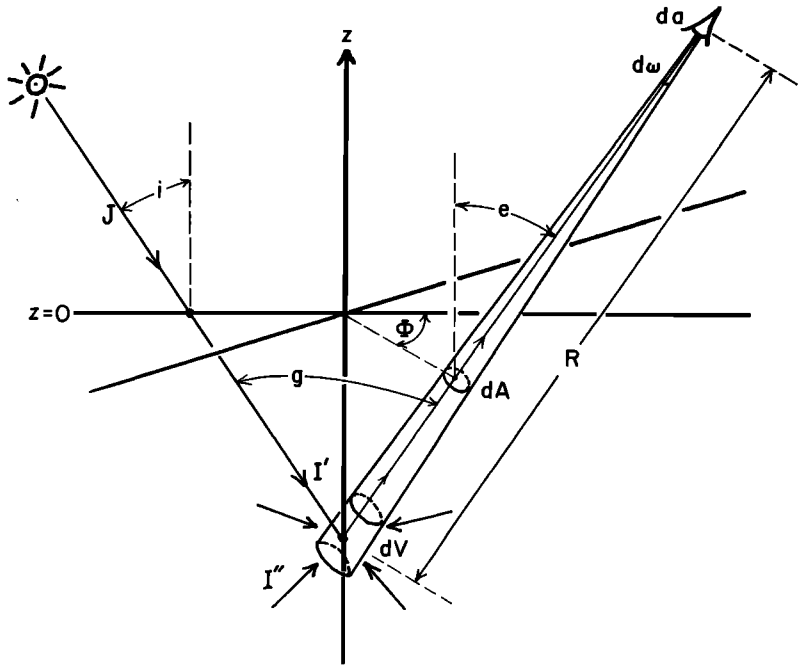

Fig. 1. Schematic diagram of the geometry used in deriving the bidirectional reflectance.

azimuth angle $\Phi = 0$; that is, the incident light is coming from a direction which makes an angle $\theta = i$ with the z-axis (Figure 1). The medium is observed by a detector with sensitive area da, located at slant distance R_0 from the $z = 0$ surface, and which accepts light from within a solid angle $d\omega$ about a direction Ω_D making an angle $\theta = e$ with the z-axis, with azimuth angle Φ and phase angle g. Let $\mu = \cos e$ and $\mu_0 = \cos i$.

Let $I(r, \Omega)$ be the spectral radiance or specific intensity. This quantity is defined as the radiant energy per unit wavelength interval at point r passing in unit time through unit area perpendicular to direction of travel per unit solid angle about the direction Ω into which the radiation is moving. The equation of radiative transfer which describes the behavior of $I(r, \Omega)$ [cf. *Chandrasekhar*, 1960] for the case of no sources imbedded in the medium is then

$$\frac{dI(r, \Omega)}{ds} = -EI(r, \Omega) + \int_{4\pi} I(r, \Omega')G(\Omega', \Omega)\, d\Omega' \qquad (1)$$

where ds is a path length parallel to Ω making an angle θ with the z-axis, E is the extinction coefficient of the medium, and $G(\Omega', \Omega)$ is the differential volume scattering coefficient which describes the probability that a photon traveling in direction Ω' will be scattered into direction Ω. For a dispersed particulate medium

$E = \sum_i N_i Q_{Ei}$;

$G(\Omega', \Omega) = \sum_i \sigma_i Q_{Si} p_i(g)/4\pi$;

S scattering coefficient of the medium, equal to $\sum_i N_i \sigma_i Q_{Si}$;

K absorption coefficient of the medium, equal to $\sum_i N_i \sigma_i Q_{Ai}$.

Here

N number of particles per unit volume;

σ average geometric cross section of particle;

Q_E extinction efficiency of particle;

Q_S scattering efficiency of particle;

Q_A absorption efficiency of particle;

$p(g)$ phase function of particles, normalized so that $\int_{4\pi} p_i(g)\, d\Omega = 4\pi$ (for isotropic scatterers, $p_i(g) = 1$);

g phase angle;

i subscript denoting particles of type i for a multicomponent medium.

The extinction efficiency includes any process which removes photons from the beam of light and includes both scattering and absorption so that $Q_{Ei} = Q_{Si} + Q_{Ai}$. Let $P(g) = 4\pi G/S$ be the average particle phase function and $N = \sum_i N_i$. The first term on the right side of (1) describes the light scattered and absorbed out of the beam as it traverses ds, while the second term describes the light scattered into the beam. These expressions also apply to molecules or to a mixture of molecules and aerosols. For molecules, the product $(\sigma_i Q_i)$ is usually not separated.

Consider a volume element, $dV = R^2\, d\omega\, dR$, located along the line of sight of the detector where this line intercepts the z-axis below the $z = 0$ surface a distance R from the detector. This element contains $N\, dV$ particles. The volume element is illuminated by both the collimated incident light I' which has penetrated between the particles to dV, and by diffuse light I'' which has been scattered one or more times by other particles. Then the intensity of light scattered by the particles in dV toward the detector is

$$d\bar{I} = \int_{4\pi} [I'(z, \Omega') + I''(z, \Omega')]G(\Omega', \Omega)\, dV\, \frac{da}{R^2}\, d\Omega'$$

Define the average single-scattering albedo

$$w = S/E \qquad (2)$$

(Author's note: *Chandrasekhar* [1960] represented the single-scattering albedo by an archaic script form of the Greek letter pi with subscript zero. Many authors, in attempting to follow this notation, use the Greek letter lowercase omega with a tilde above, which resembles the archaic pi. I have heard vari-

ous authorities refer to this symbol as 'curly-pi-sub-naught,' 'omega-tilde-sub-naught,' and 'pomega-sub-zero.' I see no compelling reason to continue this tradition and will use the less cumbersome lower case Roman w for the single-scattering albedo.) Then this integral can be written

$$d\bar{I} = \frac{w}{4\pi}\left\{\int_{4\pi}[I'(z,\Omega') + I''(z,\Omega')]P(g)\,d\Omega'\right\} E\,dR\,d\omega\,da$$

This light is attenuated by a factor $\exp[-E(R - R_0)] = \exp(Ez/\mu)$ by particles lying above the volume element along the line of sight. Thus the radiance (power per unit area per unit solid angle of the detector) reaching the detector is

$$\bar{I} = \bar{I}_s + \bar{I}_M$$

where $\bar{I}_s$ is the singly scattered radiance

$$\bar{I}_s = \frac{w}{4\pi}\int_{-\infty}^{0}\left[\int_{4\pi} I'(z,\Omega')P(g)\,d\Omega'\right] e^{Ez/\mu}\frac{E}{\mu}\,dz \qquad (3)$$

and $\bar{I}_M$ is the multiply scattered radiance

$$\bar{I}_M = \frac{w}{4\pi}\int_{-\infty}^{0}\left[\int_{4\pi} I''(z,\Omega')P(g)\,d\Omega'\right] e^{Ez/\mu}\frac{E}{\mu}\,dz \qquad (4)$$

The first integral can be evaluated exactly for any arbitrary phase function, since I' is just the collimated incident light exponentially attenuated by passage from the surface to dV:

$$I' = Je^{-Ez/\cos(\pi - i)}\delta(\theta = \pi - i)\,\delta(\Phi = 0)$$

where δ is the Dirac delta function. Thus the singly scattered contribution to $\bar{I}$ is

$$\bar{I}_S = \frac{w}{4\pi}\int_{-\infty}^{0} Je^{Ez(\mu_0^{-1}+\mu^{-1})}P(g)E\,dz/\mu = J\frac{w}{4\pi}\frac{\mu_0}{\mu_0+\mu}P(g) \qquad (5)$$

For isotropic scattering, $P(g) = 1$, and (5) is the well-known Lommel-Seeliger Law.

To evaluate $\bar{I}_M$, the two-stream approximation for isotropic scattering will be used to solve the equation of radiative transfer for light I'' which has been scattered one or more times. Equation (1) becomes

$$\frac{dI''}{ds}(z,\Omega) = -EI''(z,\Omega) + \frac{S}{4\pi}\int_{4\pi}[I'(z,\Omega') + I''(z,\Omega')]\,d\Omega'$$

Let Ω make an angle θ with the z-axis, so that $dz = ds\cos\theta$. Define the optical thickness $u = \int_0^z E\,dz$. Then this equation transforms to

$$\cos\theta\frac{dI''}{du}(u,\Omega) = -I''(u,\Omega) + \frac{w}{4\pi}\int_{4\pi}[I'(u,\Omega') + I''(u,\Omega')]\,d\Omega'$$

The two-stream solution proceeds by integrating this equation separately over the upwardgoing (U) and downwardgoing (D) hemispheres,

$$\frac{d}{du}\int_{\Omega_U} I''\cos\theta\,d\Omega = -\int_{\Omega_U} I''\,d\Omega + \frac{w}{4\pi}\int_{\Omega_U}\int_{4\pi}[I' + I'']\,d\Omega'\,d\Omega \qquad (6a)$$

$$\frac{d}{du}\int_{\Omega_D} I''\cos\theta\,d\Omega = -\int_{\Omega_D} I''\,d\Omega + \frac{w}{4\pi}\int_{\Omega_D}\int_{4\pi}[I' + I'']\,d\Omega'\,d\Omega \qquad (6b)$$

Define the average intensities for light traveling separately in the upward and downward directions, respectively, as

$$F_U = 2\pi\langle I_U''\rangle = \int_{\Omega_U} I''\,d\Omega \qquad F_D = 2\pi\langle I_D''\rangle = \int_{\Omega_D} I''\,d\Omega$$

In (6), I'' is replaced by its average over each hemisphere. Then for isotropic scatterers, (6) becomes

$$\frac{1}{2}\frac{dF_U}{du} = -\left(1 - \frac{w}{2}\right)F_U + \frac{w}{2}F_D + J\frac{w}{2}e^{\mu/\mu_0} \qquad (7a)$$

$$-\frac{1}{2}\frac{dF_D}{du} = \left(1 - \frac{w}{2}\right)F_D + \frac{w}{2}F_U + J\frac{w}{2}e^{\mu/\mu_0} \qquad (7b)$$

The solutions to (7) with the boundary conditions $F_D(-\infty) = 0 = F_U(-\infty)$ and $F_D(0) = 0$ (since there are no diffuse sources above the plane $z = 0$) are

$$F_U = J\left\{\frac{A}{1-\gamma^2}(1-\gamma)^2e^{2\gamma u} - \left[1 + \frac{A}{1-\gamma^2}\left(1 + \gamma^2 - \frac{1}{\mu_0}\right)\right]e^{\mu/\mu_0}\right\}$$

$$F_D = JA\{e^{2\gamma u} - e^{\mu/\mu_0}\}$$

where

$$A = (1-\gamma^2)\frac{(1/\mu_0) + 2}{\mu_0^{-2} - 4\gamma^2}$$

and

$$\gamma = (1 - w)^{1/2} \qquad (8)$$

Then in (4),

$$\int_{4\pi} I''(z,\Omega')P(g)\,d\Omega' = F_U(u) + F_D(u)$$

and the contribution of the multiply scattered component in the case of isotropic scatterers is

$$\bar{I}_M = \frac{w}{4\pi}\int_{-\infty}^{0}[F_U + F_D]e^{u/\mu}\frac{du}{\mu}$$

The integration is readily carried out and gives

$$\bar{I}_M = J\frac{w}{4\pi}\frac{\mu_0}{\mu_0+\mu}[H(\mu_0)H(\mu) - 1] \qquad (9)$$

where

$$H(\mu) = \frac{1 + 2\mu}{1 + 2\gamma\mu} \qquad (10)$$

Thus for isotropic scatterers the total reflected radiance from the surface is the sum of (5) and (9),

$$\bar{I}(\mu_0,\mu,g) = \bar{I}_S + \bar{I}_M = J\frac{w}{4\pi}\frac{\mu_0}{\mu_0+\mu}H(\mu_0)H(\mu) \qquad (11)$$

Chandrasekhar [1960] has obtained the exact solution of the isotropic scattering problem. His solution has the same form as (11), except that his H-functions are solutions of the integral equation

$$H(\mu) = 1 + \tfrac{1}{2}w\mu H(\mu)\int_0^1\frac{H(\mu')}{\mu+\mu'}\,d\mu'$$

which must be evaluated numerically. The approximate (equation (10)) and exact evaluations of the H-functions are compared in Figure 2, where it is seen that the two solutions agree to better than 3% everywhere.

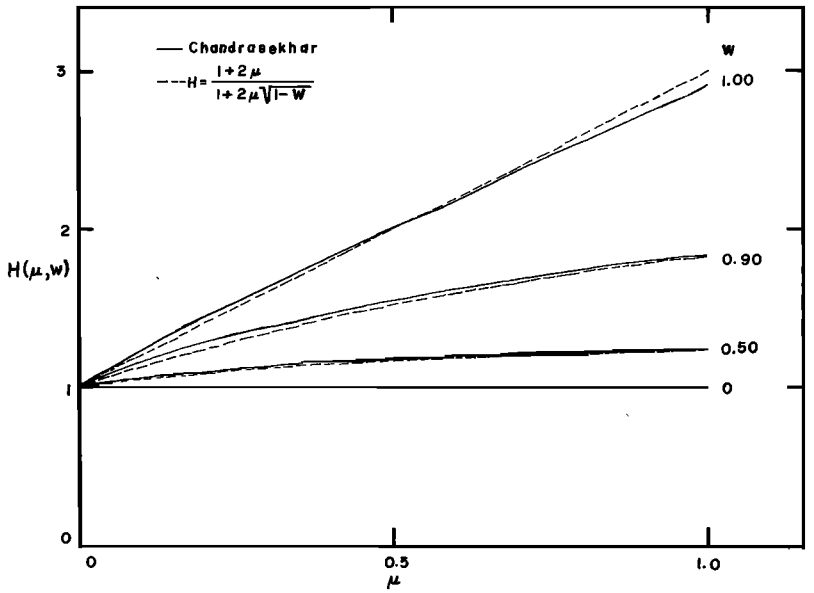

Fig. 2. The H-functions versus μ for several values of single-scattering albedo. Solid lines: Chandrasekhar's exact solutions; dashed lines: approximations of this paper.

Chandrasekhar has emphasized (see also *Hansen and Travis* [1974, Figure 27]) that for a semi-infinite medium, the multiply scattered portion $\bar{I}_m$ of $\bar{I}$ is much less sensitive to the particle phase function than the singly scattered fraction $\bar{I}_S$. The brighter the surface, the more times the average photon is scattered before emerging from the surface, causing directional effects to be averaged out and the multiply scattered intensity distribution to closely approach the isotropic case. Since the single-scattering term can be evaluated exactly for an arbitrary phase function and the multiply scattered term is relatively insensitive to phase function, a first-order expression for nonisotropic scatterers can be obtained by using the exact expression for $\bar{I}_S$ but retaining the isotropic solution for $\bar{I}_M$. Then

$$\bar{I}(\mu_0, \mu, g) = J \frac{w}{4\pi} \frac{\mu_0}{\mu_0 + \mu} [P(g) + H(\mu_0)H(\mu) - 1] \quad (12)$$

How good is this approximation for the multiply scattered contribution? As can be seen from Figure 2, the maximum contribution of I_M will occur when high-albedo surfaces are observed and illuminated nearly vertically. Figures 3, 4, and 5 compare the approximate solutions of (12) with exact numerical solutions obtained by *Chandrasekhar* [1960] for $e = 32°$, $w = 1.00$, and three phase functions: isotropic, $P(g) = 1$, back scattering, $P(g) = 1 + \cos g$, and forward scattering, $P(g) = 1 - \cos g$. Also shown are calculations for $w = 0.2$. It is seen that even for the case $w = 1$ (which is never achieved in practice) the approximation is good to better than 15%. Since the derivative of the H-function with w is infinite at $w = 1$, an extremely small decrease in w considerably reduces the disagreement (Figure 3). For example, when $w = 0.975$, the error is only 0.7%.

b. *Effects of Decreasing the Interparticle Spacing*

The discussion so far applies to a medium in which the particles are well dispersed. Moving the particles closer together until ultimately they are in contact affects the reflectance process in three ways: (1) The medium can no longer be considered continuous, (2) shadowing occurs, causing preferential escape at zero phase, and (3) diffraction ceases to be a meaningful concept. Each of these effects will now be discussed.

Effects of a discontinuous medium and shadowing. When the particles are widely dispersed so that they can be considered to scatter independently, the medium can be treated as

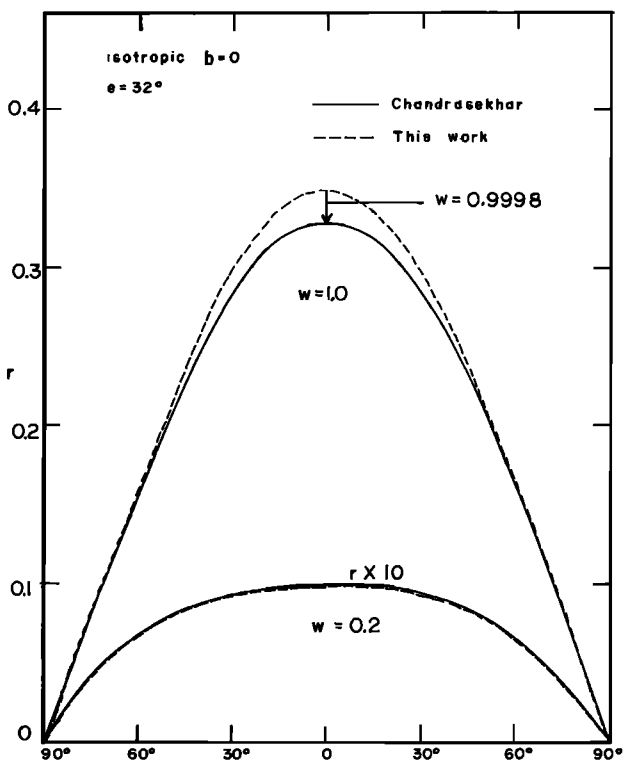

Fig. 3. Comparison of exact and approximate solutions for the bidirectional reflectance of a surface of isotropic scatterers as a function of i in a vertical plane containing the directions to the source and detector for $e = 32°$ and two values of w. A change in w from 1.0000 to 0.9998 is sufficient to bring the two solutions into nearly exact agreement.

continuous with the properties averaged as given by the definitions of E, S, and K above. When the particles are so close together that they are in contact, as in a powder or soil, coherent interference can occur between portions of waves scattered by neighboring particles. It is assumed that the particles are irregular and arranged with no particular packing or orientation, so that coherent effects average out.

When dispersed, each particle can be treated as if it is fully illuminated by ambient light. When close together, one particle may find itself partially in the shadow of another so that its full efficiency for scattering and absorption cannot be utilized. If the medium is random, then it may reasonably be assumed that light falling on a portion of a particle will, on the average, be scattered or absorbed by the same relative amount as if the particle were fully illuminated, but reduced by the fraction of the cross-sectional area illuminated. That is, it is assumed that the efficiencies are all affected by the same amount. If so, then neither w nor $P(g)$ will be changed, since they involve only ratios of the efficiencies, and (12) will not be affected.

Preferential escape—The opposition effect. The factor exp (Ez/μ_0) represents the probability that a portion of the surface of a particle at depth z will be directly illuminated by light of intensity J which has penetrated to that particular point without being blocked by another particle. Likewise, the other factor exp (Ez/μ) can be regarded as the probability that light emerging from the same area on the surface of the particle in the direction of the detector will reach the $z = 0$ plane without encountering another particle. However, it was pointed out in an earlier paper [*Hapke*, 1963] that near zero phase the two probabilities are not independent because the incident light, in effect, preselects a preferential escape path. That is, if the source happens to be positioned exactly so that incident radiation can penetrate to a certain place without being blocked, then the radiation which happens to be scattered directly back within a small angle about the source direction will reach the $z = 0$ plane without attenuation. Thus for radiation within this small angle, the escape probability is unity rather than exp (Ez/μ). This effect has also been discussed by *Irvine* [1966] and *Lumme* [1971].

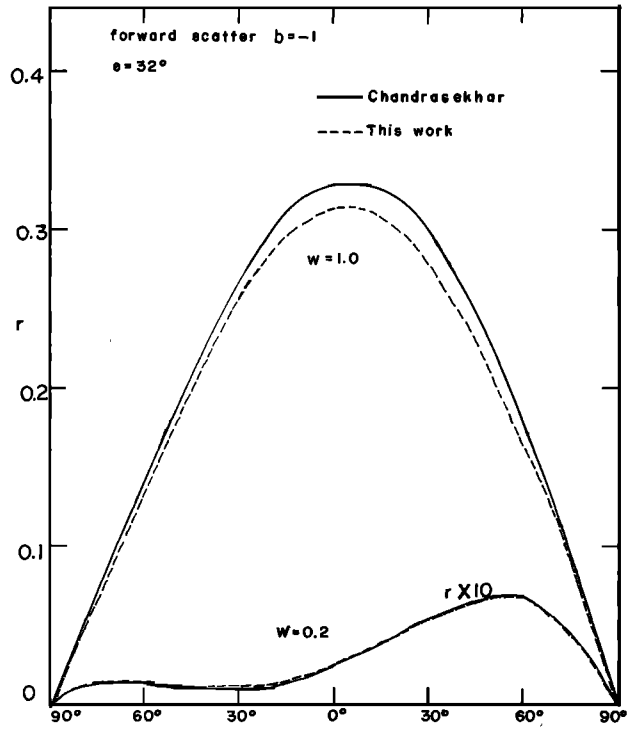

Fig. 4. Same plot as for Figure 3, except for forward scattering particles with a phase function $P(g) = 1 - \cos g$.

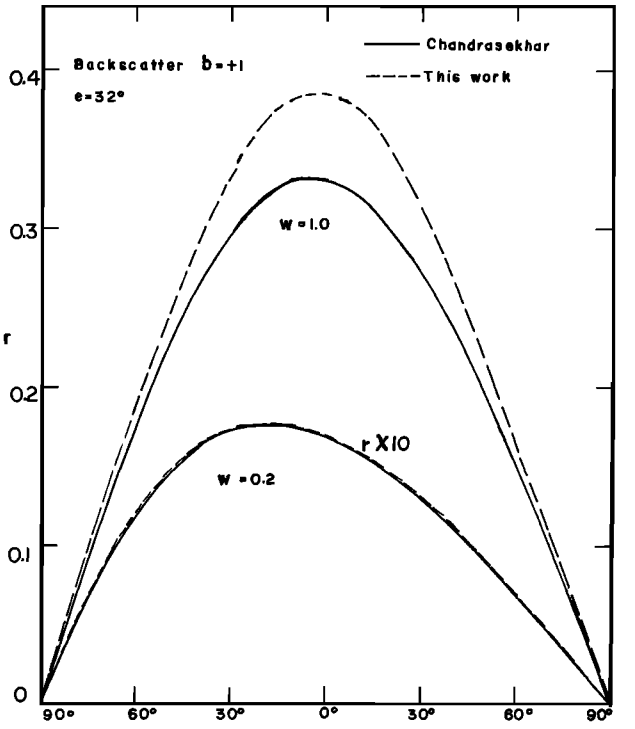

Fig. 5. Same plot as for Figure 3, except for back scattering particles with a phase function $P(g) = 1 + \cos g$.

The preferential escape applies only to the unscattered illuminating radiation I', because the multiply scattered radiation I'' bathes all the particles in a volume element uniformly and does not preselect an escape path. Thus the probability of escape for I'' scattered from any given particle statistically remains exp (Ez/μ), and $\bar{I}_M$ is unchanged. This conclusion is supported by a numerical calculation by *Esposito* [1979], who finds that including an opposition effect in second-order scattering has a negligible effect.

Hapke [1963] showed that the preferential escape of singly scattered radiation can be taken into account by a model in which the medium contains imaginary cylinders whose axes are parallel to the incident rays. The diameter of the cylinders is of the order of the mean openings between particles. Light scattered from a particle and passing through the sides of the cylinder is exponentially attenuated, but scattered light reaching the $z = 0$ plane without passing through the sides has zero attenuation. The original reference may be consulted for the details of the derivation. This model leads to a modified form for $\bar{I}_S$

$$I_S = J \frac{w}{4\pi} \frac{\mu_0}{\mu_0 + \mu} P(g)[1 + B(g)]$$

where $B(g)$ is the backscatter function

$$B(g) = 1 - \frac{\tan |g|}{2h}(3 - e^{-h/\tan|g|})(1 - e^{-h/\tan|g|}) \qquad |g| \leq \pi/2$$

$$B(g) = 0 \qquad |g| \geq \pi/2$$

h is a parameter which depends on particle spacing, $h = N\sigma Q_E y$, where y is the diameter of the equivalent circle having the same projected area as the openings between particles. (For reasons which will become apparent below, a minor change in notation from the 1963 paper has been made: $B(g)$ of the 1963 paper is replaced by $[1 + B(g)]$ here.)

The original treatment considered the scattering particles as behaving essentially as points, in the sense that all parts of the particle have the same illumination and attenuation probabilities. However, a real particle will have a finite size and usually will be situated so that only a portion of its surface is illuminated. The refracted light which penetrates into the particle will be redistributed inside the particle and re-emerge in a manner which depends on the single-scattering albedo. If a particle is dark and highly absorbing, most of the refracted light will be absorbed before it travels very far from its place of entry. Most of the light scattered from a low-albedo particle will leave from the immediate vicinity of the illuminated part of the surface, and for small phase angles the attenuation probability will be unity, as discussed above. However, for bright, weakly absorbing particles much of the scattered light will emerge from unilluminated parts of the surface which were not preselected by the incident rays, and for this light the attenuation will be exponential and will not contribute to the opposition effect. Thus the original expression for $B(g)$ must be multiplied by a factor which describes the probability that the light will exit the particle near the directly illuminated part of its surface. Such a probability cannot, in general, be calculated exactly, since it depends on such properties as particle shape, index of refraction, and density of internal scatterers and must be represented by an empirical factor B_0. Thus $B(g)$ is modified to

$$B(g) = B_0\left[1 - \frac{\tan|g|}{2h}(3 - e^{-h/\tan|g|})(1 - e^{-h/\tan|g|})\right] \quad |g| \le \pi/2$$

$$B(g) = 0 \qquad |g| \ge \pi/2 \tag{13}$$

For $|g| \ll 1$, $B(g) \simeq B_0(1 - 3|g|/2h$.

The parameter B_0 describes the magnitude of the opposition effect. For a low-albedo surface, such as the moon or Mercury, $B_0 \simeq 1$. This quantity is hard to measure uniquely in the laboratory because the experimental results depend on the degree of collimation of the incident light and angular size of the detector, as well as on the properties of the surface. In Paper II, results are reported using a photometer for which the angular diameter of both source and detector is about 0.5° as seen from the surface. Under these conditions it appears possible to represent the amplitude of the opposition effect for fine particles crudely by

$$B_0 \approx e^{-w^2/2} \tag{14}$$

This expression is probably descriptive of most planetary regoliths.

For what particle spacings is the opposition effect important? A powder with a small dispersion in sizes will have $\pi y^2/4 = L^2 - \sigma$, where $L = N^{-1/3}$ is the mean spacing between particle centers. Thus for approximately spherical particles with a narrow dispersion of sizes,

$$h = L^{-3}\frac{\pi}{4}D^2Q_E\left[\frac{4}{\pi}\left(L^2 - \frac{\pi}{4}D^2\right)\right]^{1/2}$$

$$= Q_E\frac{\pi}{4}\left(\frac{D}{L}\right)^2\left[\frac{4}{\pi} - \left(\frac{D}{L}\right)^2\right]^{1/2}$$

This parameter is double-valued, having a broad maximum at $D/L = 0.8$ and $h = 0.43$. Particles in contact with $Q_E = 1$ (see below) and $L \simeq D$ have $h \simeq 0.4$. Compacted powders with a large distribution of particle sizes will have h smaller than 0.4 because smaller particles fill in the spaces between larger particles, increasing D/L. Thus the typical laboratory powders described in Paper II have $h \sim 0.1$–0.2. Uncompacted lunar soil in its natural state has $h = 0.4$ [*Hapke,* 1966].

Starting with a compacted surface, as the porosity increases and the particles move farther apart, h first increases and then decreases, and the backscatter function narrows. Since the opposition effect depends on sharp shadows, eventually it disappears when the particles are so far apart that few of them are in the umbra of each other's shadows. The fraction of the volume occupied by the umbras is $N\sigma D/3\theta_s$, where θ_s is the angular diameter of the source. Thus the opposition effect disappears when $N\sigma D/3\theta_s = (\pi/12\theta_s)(D/L)^3 \ll 1$, say, 0.1. This requires

$$L/D \gtrsim 1.4\theta_s^{-1/3}$$

At 1 AU, $\theta_s \sim 0.01$ and the critical $L = 7D$. At 10 AU, $\theta_s \sim 0.001$ and the critical $L = 14D$. Since $B(g)$ disappears for moderate separations, it is difficult to imagine that the pronounced opposition effect displayed by Saturn's rings is due to mutual shadowing by separate ring particles. More likely, it is a property of the particles themselves, as discussed by *Price* [1974]. The presence or absence of an opposition effect on a planet can be used to deduce whether the scattered light comes from a regolith or clouds [*Veverka,* 1974].

In the literature the magnitude of the opposition effect is usually measured as the ratio of the brightness of a surface at a phase angle as small as can be used (typically 1°) to the brightness at a larger phase angle (typically 5° to 30°, depending on the author). Defined in this way, the opposition effect is strongly dependent on albedo, in agreement with observations [*Hapke,* 1968; *O'Leary and Jackel,* 1970; *Egan and Hilgeman,* 1976] because the effect operates only on a fraction B_0 of the singly scattered radiation.

Diffraction. All isolated particles large compared with the wavelength scatter light strongly into a narrow cone in the forward direction, and relatively weakly in other directions. For roughly spherical particles this forward-scattering lobe can be identified with the Babinet diffraction pattern of an isolated opaque disk [*Van de Hulst,* 1957; *Kerker,* 1969; *Hodkinson and Greenleaves,* 1963] and can be separated mathematically from the large-angle scattering. Thus the particle scattering function can be written

$$Q_sP(g) = Q_s'P'(g) + Q_s''P''(g)$$

where the single prime refers to the large-angle component of the scattering which is not associated with diffraction and the double primes refer to the small-angle, diffracted component. Q_s' and $P'(g)$ depend on the size, shape, and composition of the particle, but for approximately spherical particles, $Q_s'' = 1$, and

$$P''(g) = 4J_1^2[X\sin(\pi - g)]/[\sin(\pi - g)]^2 \tag{15}$$

where $X = \pi D/\lambda$ and $J_1(x)$ is the Bessel function of first order and argument x.

Widely separated particles have $Q_E \simeq 2$ because the amount of area of the impinging wavefront which is appreciably perturbed by the particle is approximately twice the geometric cross-section σ. The diffracted component can be considered

as arising mainly from light which passes between the edge of the particle and a distance $D/(2)^{1/2}$ from the center, making $Q_s'' = 1$. However, when the particles are close together, their diffraction-source areas overlap, and the amount of light diffracted by each particle decreases. Ultimately, when the particles are in contact, each monolayer can be considered as consisting either of random disks in an infinite, open plane or of random holes in an infinite screen. Since the total amount of light transmitted by an opaque screen with holes cannot exceed the fraction impinging on the holes, the effective Q_E of each particle cannot exceed unity, which requires that $Q_s'' = 0$.

Another way of looking at this effect is to consider a detector located well behind a particle, within the cone of diffracted light. Then the detector will measure an excess of light which it interprets as having been scattered from the particle. If the detector is moved so that it is only slightly behind and to one side of the particle, within the geometric 'shadow' of the diffraction-source area, it will detect the light which would have been scattered into the diffraction cone, but which is spread out by such a small amount that it essentially has the same intensity as the incident illumination; this light is now interpreted as unscattered incident light. In a close-packed powder the underlying particles function as 'detectors' of the diffracted light from other particles. The diffracted light must be treated as being indistinguishable from unscattered incident light, so that $Q_s = Q_s'$ and $Q_E = 1$.

The half-width θ'' of the diffraction cone is given by $\pi D(\sin\theta'')/\lambda = 1.62$ or $\theta'' \simeq \lambda/2D$, the diffracted light coming from rays which pass within a distance $D/(2)^{1/2}$ of the particle. Thus particles which are situated within a distance $L'' \sim D/(2)^{1/2}\theta'' = (2)^{1/2}D^2/\lambda$ behind the first particle will be illuminated by light which has not been attenuated appreciably by spreading. Particles at a distance much greater than L'' behind the first particle will be illuminated by light which is already spread well into its diffraction cone and will interpret this light as having been scattered. Of the light scattered into the diffraction cone, a fraction $\exp(-N\sigma L'')$ will have been transmitted without being intercepted by closer particles and can be considered as having been diffracted, while the remainder, $1 - \exp(-N\sigma L'')$, can be treated as incident light. Thus the condition for neglecting diffraction is $\exp(-N\sigma L'') \ll 1$, or say,

$$N\sigma L'' = \frac{\pi}{2(2)^{1/2}}\left(\frac{D}{L}\right)^3 \frac{D}{\lambda} \gtrsim 5$$

or $L/D \lesssim 0.6(D/\lambda)^{1/3}$. For particles nearly in contact ($L \simeq D$) this condition is met by all particles larger than a few wavelengths, while for particles much smaller than this the concept of a separable diffraction component breaks down anyway.

The changing role of diffraction with interparticle distance may account for the common observation that the reflectance of a powder changes somewhat with particle density [*Blevin and Brown*, 1961] (see also paper II). The reflectance of a dark powder decreases slightly as the concentration decreases and spacing increases. The relative change decreases with increasing albedo, until for very bright powders the reflectance may actually increase slightly. For low-albedo powders the reflectance is dominated by the single-scattering term $\bar{I}_S$ and is proportional to $wP(g)$. When the interparticle separation is small, $Q_E \simeq 1$, $Q_S \simeq Q_S'$, and $wP(g) \simeq Q_S'\,P'(g)$. As the separation increases and diffraction becomes important, $Q_E \simeq 2$, and $wP(g)$ changes to $[Q_S'P'(g) + P''(g)]/2$. But $P''(g)$ contributes to the intensity only at very large phase angles, so that the brightness at small phase angles drops. For bright surfaces the reflectance is dominated by the multiply scattered term $\bar{I}_M \propto [H(\mu)H(\mu_0) - 1]$, which increases slightly as w changes from Q_S' to $(Q_S' + 1)/2$.

c. *The Bidirectional Reflectance*

Collecting the results of section 2, the bidirectional reflectance $r = \bar{I}/J$ of a surface consisting of particles of arbitrary shape in close proximity to one another is given to a good approximation by

$$r(\mu_0, \mu, g) = \frac{w}{4\pi}\frac{\mu_0}{\mu_0 + \mu}\{[1 + B(g)]P(g) + H(\mu_0)H(\mu) - 1\} \quad (16)$$

where $B(g)$ is the backscattering function given by (13), $H(\mu)$ is a multiple-scattering function given by (10), and w is the average single-scattering albedo and is computed from (2) neglecting diffraction in Q_S and Q_E. Surfaces containing abundant fine particles have an opposition effect characterized by $h \sim 0.1$–0.4 and $B_0 \sim \exp(-w^2/2)$.

Multimineralic media. The reflectance is governed by w. If the particles are spherical, the bulk density M_i of particles of type i with diameter D_i and solid density ρ_i is $M_i = N_i\rho_i\pi D_i^3/6$, and their cross-sectional area is $\sigma_i = \pi D_i^2/4$. Then $N_i\sigma_i = 3M_i/2\rho_iD_i$. If the particles are large compared with the wavelength and are close together, $Q_{Ei} = 1$, and w can be written

$$w = S/E = \left(\sum_i \frac{M_i}{\rho_iD_i}Q_{Si}\right)\Big/\left(\sum_i \frac{M_i}{\rho_iD_i}\right) \quad (17)$$

If the particles are not spherical, a different geometrical factor than 3/2 appears in $N_i\sigma_i$. However, (17) is still applicable, provided the particles all have approximately the same shape.

3. SINGLE-PARTICLE SCATTERING

a. *Discussion*

Frequently in reflectance photometry it is desired to calculate the reflectance of a surface from the absorption coefficient α or, conversely, to estimate quantitatively the spectral absorption coefficient α of a planetary surface material from measurements of the reflectance of the regolith. This goal requires a relationship between α and w. Unfortunately, no adequate theory exists which relates the complex index of refraction, particle size, and single-scattering albedo, except for particles of extremely simple shapes. In this section the general problem of scattering from a large, irregular particle is reviewed, and some useful semi-empirical relationships are derived.

The general problem of the scattering of a plane electromagnetic wave from a perfect sphere can be solved exactly and is referred to as Mie theory. A number of calculations of Mie efficiencies and phase functions have been published in the literature, including *Van de Hulst* [1957], *Kerker* [1969], *Deirmendjian* [1969], *Hansen and Travis* [1974], and many others.

The solutions are generally expressed in terms of the size parameter $X = \pi D/\lambda$ and the complex index of refraction (relative to the surrounding medium, usually a vacuum)

$$m = n(1 - jk) \quad (18)$$

where $j = (-1)^{1/2}$. The volume absorption coefficient α is related to the imaginary component of the refractive index through the dispersion relation

$$\alpha = 4\pi nk/\lambda \quad (19)$$

The case when $X \ll 1$ is called the Rayleigh region. There [*Kerker*, 1969] $Q_S \propto X^4$, $Q_A \propto kX$, and $P(g) \propto (1 + \cos^2 g)$. As X increases through unity, the efficiencies of the sphere oscillate strongly. As X becomes large compared with one, Q_E oscillates about 2 with decreasing amplitude; the scattering functions all exhibit strong forward scattering associated with diffraction, as discussed previously, plus a moderate backscattering peak, known as the glory. The scattering function tends to be low for phase angles around 90°, and there are often other peaks, known as cloudbows, at specific angles. Many of these properties can be duplicated by calculations of rays reflected from and refracted through surfaces of the sphere, plus the diffraction term.

The particles of most materials of planetary interest have an irregular shape. An exact calculation of scattering from such particles is presently out of the question. Large, nonspherical particles can be treated by a Monte Carlo ray calculation, plus diffraction, but this requires an elaborate computer program.

A number of experimental studies have been made using artificial models at microwave frequencies and naturally occurring particles at optical wavelengths [*Zerull*, 1976; *Giese and Zerull*, 1974; *Zerull and Giese*, 1974; *Zerull et al.*, 1977; *Hodkinson*, 1963; *Chylek et al.*, 1976]. The results of the studies show that the scattering from an irregular particle is roughly similar to the scattering from a similar sized sphere predicted by Mie theory, in that the efficiencies are comparable. However, large, irregular particles do not have glories or cloudbows; the minimum near $g = 90°$ disappears (that is, the scattering function is approximately isotropic, except for the diffraction lobe); also, the oscillations of the efficiencies near $X = 1$ disappear and Q_E rises smoothly to 2.

Similar conclusions are implied by astrophysical observations. Interplanetary dust particles presumably are irregular. Analyses of light scattered by cometary dust by *Ney and Merrill* [1976] indicate that the interplanetary microparticles scatter approximately isotropically outside the diffraction lobe.

Inspection of Apollo samples shows that lunar soil particles are irregular. *Hapke* [1963] showed that the average single-particle scattering function of the lunar surface can be represented by

$$P(g) = \frac{4\pi}{5}\left[\frac{\sin g + (\pi - g)\cos g}{\pi} + \frac{(1 - \cos g)^2}{10}\right]$$

which is nearly isotropic except for wide, moderate lobes in the forward and backward directions. No diffracted component was necessary in the lunar function, consistent with the discussion of this paper.

Thus the assumption that large, closely-spaced, irregular particles scatter approximately isotropically would appear to be well justified. A second-order expansion of the scattering function in Legendre polynomials

$$P(g) = 1 + bP_1(g) + cP_2(g) \tag{20}$$

where $P_1(g) = \cos g$ and $P_2(g) = (3\cos^2 g - 1)/2$ are Legendre polynomials, should be adequate for most particulate surfaces. Thus (16) should be an excellent approximation for describing scattering from most laboratory or planetary surfaces.

It should be pointed out that soils which have abundant particles small compared with the wavelength will be extremely cohesive. The submicroscopic particles will stick to the surfaces of larger particles or clump together into large aggregates and thus will behave like irregular particles with $X \gg 1$ and strong internal scattering.

Large particles may have a complex surface structure which is small compared to D but large compared to λ, for example, a scoriaceous lava. The effect of surface irregularities depends on their size compared with α^{-1}. If their scale is small compared with α^{-1}, they will not cast dark shadows, and the phase function of the particle will remain approximately isotropic. This would be the case, for instance, for 10-μm irregularities on 0.1- to 1-mm silicate particles, as in lunar soils. However, if the irregularities have sizes which are comparable with or larger than α^{-1}, they will cast deep shadows. The surface pits will then cause $P(g)$ to have a rather strong backscattering character which will add to the opposition effect discussed in (2*b*). The latter case may characterize Saturn's rings.

b. Theoretical Scattering Efficiency for Large, Irregular Particles

One of the problems of reflectance spectroscopy is to relate the measured brightness, from which w can be calculated, to the microscopic quantities n, k, and D. The quantity which is usually of greatest interest is the volume absorption coefficient $\alpha = 4\pi nk/\lambda$. In the following discussion it is assumed that the particles are large compared with the wavelength and are closely spaced, as in a laboratory powder or planetary regolith. Then $Q_E = 1$, diffraction may be ignored, and a ray model is appropriate.

Scattering from a large particle takes place by two processes, reflection from the surface of the grain, and internal or volume scattering of rays which have been refracted into the interior of the grain and scattered or refracted back out. The volume scattering may occur from internal imperfections, such as crystal boundaries, micro-inclusions, bubbles, and density striations, or by internal reflection from the particle surface.

Slab model. An approximate model of scattering from a large, equant particle, which takes account of both surface and volume scattering and volume absorption, will now be derived. Collimated light incident on a particle with randomly oriented surface facets will be approximated by diffuse light incident on one side of a slab with plane surfaces. The amount of light reflected and transmitted by an infinite slab with absorbers and isotropic scatterers included between the upper and lower surfaces will be calculated using the two-stream method. The calculation will then be extended to the case of equant particles.

Let S_E be the external surface scattering coefficient; S_E is the coefficient for specular, or Fresnel, reflection from the surface of the particle averaged over all directions of incidence on one hemisphere of the external surface. *Van de Hulst* [1957] has pointed out that an ensemble of randomly oriented, convex particles (that is, particles having no depressions or cavities on their surfaces) will have the same external surface scattering coefficient as spheres. For collimated light incident on the surface of a large sphere [*Kerker*, 1969],

$$S_E = \int_0^{\pi/2} [f'(\theta) + f''(\theta)] \sin\theta \cos\theta \, d\theta \tag{21}$$

where $f'(\theta)$ and $f''(\theta)$ are the Fresnel coefficients

$$f'(\theta) = |\sin(\theta - \theta')/\sin(\theta + \theta')|^2$$

$$f''(\theta) = |\tan(\theta - \theta')/\tan(\theta + \theta')|^2$$

$$\theta = g/2 \qquad \sin\theta = m\sin\theta'$$

An expression identical to (21) applies to the case of diffuse light incident on a plane surface.

A useful approximation to S_E for $1.2 \lesssim n \lesssim 2.2$, which covers many values of interest in planetary applications, is

$$S_E = \left[\frac{(n-1)^2 + (nk)^2}{(n+1)^2 + (nk)^2} + 0.05 \right] \tag{22}$$

The first term in this expression is the Fresnel reflection coefficient for normal incidence. Expressions (21) and (22) for S_E are plotted as a function of n for $k^2 \ll 1$ in Figure 6.

Let S_I be the internal surface scattering coefficient for light internally incident on the surface of the particle. For a smooth-surfaced particle of regular shape, such as a slab, cylinder, or sphere, and negligible internal scattering, the angle from the local normal at which a refracted ray is incident on an interior surface is the same as that with which it first emerged into the interior of the particle, so that $S_I = S_E$. However, if the particles are irregular or have a high density of internal scatterers, S_I will be larger than S_E because many of the internally incident rays will exceed the critical angle. It is assumed that the flux inside the grain is approximately isotropic; in that case, S_I is equal to the Fresnel coefficient for internal reflection averaged over all directions of incidence and can be calculated from (21) by replacing m by m^{-1}. Figure 6 shows S_I versus n for $k^2 \ll 1$.

Consider a slab of thickness D, with one surface at $z = 0$ and the other at $z = -D$, surface scattering coefficients S_E and S_I, internal scattering coefficient s, and internal absorption coefficient $\alpha = 4\pi nk/\lambda$. The radiation field inside the slab is described by the two-stream equations (7), with the collimated source terms $J \exp(u/\mu_0)$ set equal to zero, and w replaced by $s/(s + \alpha)$. Diffuse light of intensity F_0 is incident from above on the $z = 0$ surface. The boundary conditions, which take account of light transmitted through the upper surface and also reflected at the upper and lower surfaces, are $F_U(-D) = S_I F_D(-D)$ and $F_D(0) = (1 - S_E)F_0 + S_I F_U(0)$.

The scattering efficiency Q_S is the fraction of F_0 scattered from the upper surface plus the internal flux refracted through both the top and bottom surfaces. This leads to

$$Q_S = S_E + \frac{(1 - S_E)(1 - S_I)\{r_1 + \exp[-2(\alpha(\alpha + s))^{1/2} D]\}}{1 - r_1 S_I + (r_1 - S_I)\exp\{-2[\alpha(\alpha + s)]^{1/2} D\}} \tag{23}$$

where

$$r_1 = \frac{1 - [\alpha/(\alpha + s)]^{1/2}}{1 + [\alpha/(\alpha + s)]^{1/2}}$$

is the bihemispherical reflectance of a semi-infinite medium with absorption and scattering coefficients α and s, respectively.

Extension to an equant particle. *Melamed* [1963] has calculated the scattering efficiency of a spherical particle of diameter D with no internal scatterers and whose surface elements reflect and refract light diffusely into all directions. His expression is (to second order in αD)

$$Q_S = S_E + \frac{(1 - S_E)(1 - S_I)e^{-2\alpha D/3}}{1 - S_I e^{-2\alpha D/3}}$$

Comparison of (23) for a slab with Melamed's equation shows that when $s = 0 = r_1$, the two expressions are equal except for a factor 3 in the exponents. Now, the average path length for diffuse light in a slab is $2D$, while the average path length for diffuse light in a sphere is approximately $2D/3$ [*Melamed*, 1963]. This suggests that (23) may be made applicable to particles of any shape by an appropriate choice of the path length to take account of edge effects. Melamed's calculation suggests that the appropriate path length for equant particles is $2D/3$. This assumption will be adopted here and justified empirically in paper II. Thus the final expression for the scattering efficiency of an irregularly shaped grain is

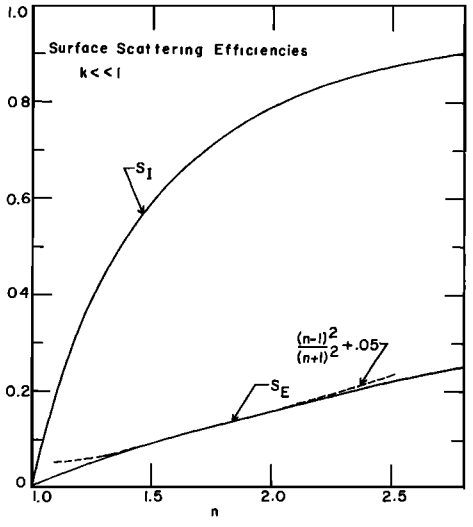

Fig. 6. Surface reflection coefficients for hemispherically integrated light versus refractive index for light externally incident (S_E) and internally incident (S_I) on the grain surface; $k \ll 1$. Dashed line is the specular coefficient for normal incidence + 0.05.

$$Q_S = S_E + \frac{(1 - S_E)(1 - S_I)\{r_1 + \exp[-2(\alpha(\alpha + s))^{1/2} D/3]\}}{1 - r_1 S_I + (r_1 - S_I)\exp\{-2[\alpha(\alpha + s)]^{1/2} D/3\}} \tag{24}$$

In the case where the grain is optically thin ($[\alpha(\alpha + s)]^{1/2} D \ll 1$), (24) becomes

$$Q_S \simeq 1 - \frac{2}{3}\frac{1 - S_E}{1 - S_I}\alpha D \tag{25}$$

In the case where the grains are optically-thick ($[\alpha(\alpha + s)]^{1/2} D \gg 1$), (24) reduces to

$$Q_S \simeq S_E + \frac{(1 - S_E)(1 - S_I)r_1}{1 - S_I r_1} \tag{26}$$

which can be further simplified to

$$Q_S \simeq S_E + (1 - S_E)(1 - S_I)\frac{s}{4\alpha} \tag{27}$$

when $s \ll \alpha$.

The importance of the internal volume scattering is clear from the last equation. Even when the absorption optical thickness αD of the particle is very large, a nonnegligible amount of light which is volume-scattered from the interior of the particle can contribute to the scattering efficiency. Thus features in the absorption spectrum of the material can still be detected in a soil of low albedo.

When $k \gtrsim 0.1$ (as is the case for metallic Fe, magnetite, and ilmenite), the particle becomes opaque, then

$$Q_S = S_E \qquad Q_S P(g) = [f'(g/2) + f''(g/2)]/2 \tag{28}$$

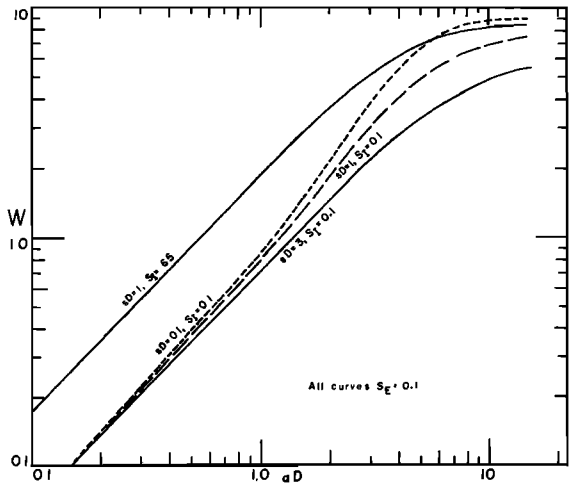

Fig. 7. Espat-function W as a function of αD for several parameters of (24).

where S_E, f', and f'' are given by (21). Note that the surface $P(g)$ is forward scattering when $k \ll 1$ but becomes isotropic as k increases. Also, this Q_S is independent of particle size.

c. *The Espat-Function and a Simplified Scattering Efficiency*

The difficulty with applying (24) for Q_S is its cumbersomeness and also the large number of parameters (S_E, S_I, s, α, and D) which must be known in order to calculate Q_S. In most applications, these parameters can only be guessed at. Therefore it would be useful to find a function which has even an approximately linear relationship with α.

Consider the function

$$W = (1 - w)/w = (E - S)/S = K/S \tag{29}$$

where w can be deduced from measurements of the reflectance of a surface using (16) or other appropriate expressions developed in section 4.

For a surface which consists of closely spaced, large particles of only one type, $w = Q_S$ and

$$W = (1 - Q_S)/Q_S \tag{30}$$

The properties of the monomineralic W-function are illustrated in Figure 7, where $w = (1 - Q_S)/Q_S$ is plotted as a function of αD for $S_E = 0.10$ and several values of the parameters S_I and s. All curves are linearly proportional to αD for small values of W and saturate at $W = (1 - S_E)/S_E$. However, the extent of the linear region depends on S_I and s. From Figure 6 it is seen that the value of n corresponding to $S_E = 0.10$ is $n = 1.60$. If the particle is smooth surfaced and has few internal scatterers $S_I = 0.10$ also. Figure 7 shows a curve for $S_I = S_E = 0.10$ and $sD = 0.10$. As the internal scattering parameter sD increases, the curve straightens and the linear range is extended. Figure 7 also shows the effect of large internal reflection. According to Figure 6, an irregular particle of $n = 1.6$ with internal scatterers will have $S_I = 0.65$. Figure 7 shows that increasing the internal surface scattering S_I increases Q_S and extends the range of linearity out to $\alpha D \simeq 3$.

Thus for $\alpha D \lesssim 3$, W is linearly proportional to αD to a good approximation. From (25) it is seen that for a monomineralic substance

$$W = \alpha D_e \tag{31}$$

where

$$D_e = \frac{2}{3}\,\frac{1 - S_E}{1 - S_I}\,D \tag{32}$$

Therefore W may be referred to as the effective single-particle absorption thickness, or espat-function.

As Figure 7 shows, even when αD is as large as 10, the error involved in assuming $W = \alpha D_e$ is only 50%, which is acceptable in many applications where only an order of magnitude estimation of α is desired. A surface with $\alpha D_e = 3$ has a normal albedo of 6%. Thus (31) should apply to all but the darkest surfaces, for which (28) must be used. The W-spectrum of a nonopaque substance obtained from the reflectance spectrum of the material in fine powder form is thus seen to be equivalent to an absorbance spectrum obtained by transmission. *Wells and Hapke* [1977] have used this result to measure absorption coefficients in strongly absorbing silicate glasses. Because n is not a strongly varying function of λ, except in the vacuum-UV or far-IR, S_E and S_I can usually be taken as constants. Provided $k^2 \ll 1$, D_e/D is not very sensitive to composition, ranging from 1.1 for $n = 1.3$ to 2.7 for $n = 2$. Thus in the absence of quantitative information on the refractive index, an estimate of $D_e \sim 2D$ is appropriate.

Combining (30) and (31) gives

$$Q_S = (1 + \alpha D_e)^{-1}. \tag{33}$$

This expression provides an extremely useful way of estimating the scattering efficiency of a grain. From a knowledge of the absorption spectrum of a substance equation (33) can be used together with equation (16) to calculate the reflectance spectrum of the material in powder form for any grain size. The reflectance of a mixture of several materials of types i can be calculated from (17) for w using $Q_{Si} = (1 + \alpha_i D_{ei})^{-1}$.

4. PLANETARY AND LABORATORY APPLICATIONS

In this section, expressions for several types of albedos and reflectances commonly encountered in planetary and laboratory applications are calculated from the preceding equations. In keeping with the philosophy expressed at the beginning of the paper, the emphasis will be on developing approximate, useful relations, rather than mathematical rigor. For completeness and convenience, the bidirectional reflectance is listed again. As above, $\gamma = (1 - w)^{1/2}$, where $w = S/E = S/(S + K)$ is the average single-scattering albedo.

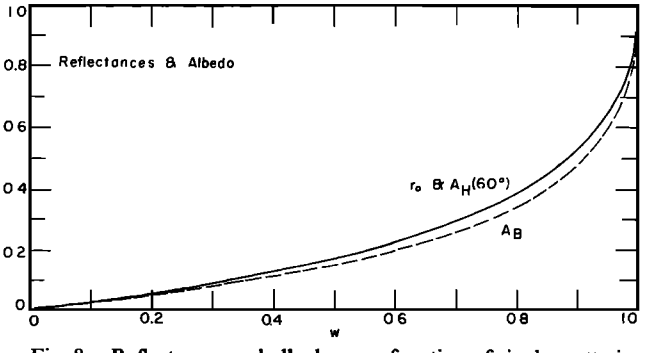

Fig. 8. Reflectances and albedos as a function of single-scattering albedo. Solid line: bihemispherical reflectance r_0, also equal to the hemispherical albedo (directional-hemispherical reflectance) A_H for $i = 60°$; dashed line: Bond albedo.

a. The Bihemispherical Reflectance r_0

The bihemispherical reflectance, or Kubelka-Munk equation [*Kubelka,* 1948; *Kottler,* 1964; *Wendtland and Hecht,* 1966; *Kortum,* 1969] is the ratio of total light scattered in all directions from a surface to uncollimated light incident on the surface. It is derived from the two-stream approximation to the equation of radiative transfer (equation (7)) with the collimated source $J \exp(u/\mu_0)$ set equal to zero and the boundary conditions $F_U(-\infty) = 0 = F_D(-\infty)$, and $F_D(0) = F_0$ = the incident flux. This gives for isotropic scatterers

$$r_0 = (1 - \gamma)/(1 + \gamma). \tag{34}$$

Although r_0 can never be measured in practice, under certain conditions other types of reflectances, including the directional-hemispherical reflectance and the radiance coefficient, are formally equal to it (see below). This fact, combined with its mathematical simplicity, makes r_0 very useful in reflectance spectroscopy. Figure 8 shows r_0 as a function of w.

A quantity related to the bihemispherical reflectance is the remission fucntion $f(r_0)$, defined as

$$f(r_0) = (1 - r_0)^2/2r_0$$

Direct substitution shows that $f(r_0) = 2K/S$. Thus except for a factor of 2 the remission function is identical to the espat-function. (Historically, the factor of 2 occurs because in the original derivation of r_0, only scatterings in which the photon is deflected by more than 90° are considered to contribute to S.) Considerable confusion exists in the literature as to the physical meaning of S in $f(r_0)$. The present discussion clarifies this point.

b. The Bidirectional Reflectance $r(\mu_0, \mu, g)$

The bidirectional reflectance is the ratio of the radiant power received per unit area per unit solid angle by a detector viewing a surface from a specific direction $e = \cos^{-1}\mu$, the surface being illuminated from a specific direction $i = \cos^{-1}\mu_0$ by collimated light, to the radiant power per unit area from the source. From (16),

$$r(\mu_0, \mu, g) = \frac{w}{4\pi}\frac{\mu_0}{\mu_0 + \mu}\{[1 + B(g)]P(g) + H(\mu_0)H(\mu) - 1\} \tag{16'}$$

where $B(g)$ is defined in (13) and $H(\mu)$ in (10). If the particles are closely spaced as in a powder or soil, diffraction is ignored in calculating w.

c. Lambert Reflectance r_L

By definition, a Lambert surface appears equally bright when viewed from any angle and reflects all the light incident on it. It is straightforward to show that this leads to

$$r_L = \mu_0/\pi \tag{35}$$

There are a number of different kinds of reflectances, including the normal albedo, physical albedo, radiance factor, and radiance coefficient, defined relative to the Lambert reflectance.

d. The Radiance Factor r_F

The bidirectional radiance factor is the brightness of a surface illuminated and viewed at arbitrary angles relative to the brightness of a Lambert surface illuminated normally:

$$r_F = \frac{w}{4}\frac{\mu_0}{\mu_0 + \mu}\{[1 + B(g)]P(g) + H(\mu_0)H(\mu) - 1\} \tag{36}$$

e. The Radiance Coefficient r_C

The bidirectional radiance coefficient is the brightness of a surface relative to the brightness of a Lambert surface identically illuminated:

$$r_C = \frac{w}{4}\frac{1}{\mu_0 + \mu}\{[1 + B(g)]P(g) + H(\mu_0)H(\mu) - 1\} \tag{37}$$

It is trivial to show that when $i = e = 60°$ and g is large enough that $B(g) = 0$, a surface of isotropic particles will have $r_C = r_0$.

f. The Normal Albedo A_N

The normal albedo is the brightness of a surface viewed at zero phase and illuminated at an arbitrary angle relative to a Lambert surface viewed and illuminated normally:

$$A_N = r(\mu_0, \mu_0, 0)/r_L(\mu_0 = 1) = \frac{w}{8}\{[1 + B_0]P(0) + H^2(\mu_0) - 1\} \tag{38}$$

For low-albedo surfaces, such as the moon, where multiple scattering is unimportant, $H^2(\mu_0) \simeq 1$ and A_N is independent of angular position on the disk.

g. The Directional-Hemispherical Reflectance (Hemispherical Albedo) A_H

The directional-hemispherical reflectance is the ratio of the radiant power emitted from a surface in all directions to the irradiance of light from a collimated source incident from a specific direction. This is the quantity which is usually measured with an integrating sphere and is important in considerations of local heat balance on a planetary surface:

$$A_H = \frac{1}{\mu_0 J}\int_{\Omega_u} Y(\mu_0, \mu, g)d\Omega = \frac{2\pi}{\mu_0 J}\int_0^1 Y(\mu_0, \mu, g)\,d\mu \tag{39}$$

where $Y(\mu_0, \mu, g) = \mu\bar{I}(\mu_0, \mu, g)$ is the power radiated into unit solid angle per unit area of the surface.

It will first be shown that the contribution of the backscattering function $B(g)$ to A_H is negligible because of the narrowness of the peak. The half-width at half-maximum of $B(g)$ occurs at $h/\tan g' = 2.74$, or $g' \simeq h/3 = 0.13$ for $h = 0.4$. Thus the contribution of the backscatter term integrated over solid angle will be of the order of $\pi(g')^2$. The relative contribution is greatest for low-albedo surfaces for which this term is about 0.005, as compared with the other terms in the expression for Y, which contribute of order 2π. Thus $B(g)$ may be set equal to zero in calculating A_H.

Equation (39) will first be evaluated for isotropic scatterers. The integral may be evaluated in two ways. One way is to note that the total power escaping per unit area from the upper surface is

$$2\pi\int_0^1 I_U''(u = 0)\mu\,d\mu = F_U(0)\int_0^1 \mu\,d\mu = F_U(0)/2$$

This gives

$$A_H = \frac{1 - \gamma}{1 + 2\mu_0\gamma} = r_0\frac{1 + \gamma}{1 + 2\mu_0\gamma} \tag{40}$$

The second way is to note that the H-functions, as defined by (10), are very similar (Figure 2) to Chandrasekhar's H-

functions and to take over bodily some of the properties deduced by him for these functions. *Chandrasekhar* [1960] showed that the average value of an H-function is

$$\langle H \rangle = \int_0^1 H(\mu)\, d\mu = \frac{2}{1+\gamma}$$

and thus from Chandrasekhar's integral equation for the H-functions

$$\int_0^1 \frac{H(\mu)}{\mu_0+\mu}\,\mu\, d\mu = \int_0^1 H(\mu)\left(1 - \frac{\mu_0}{\mu_0+\mu}\right) d\mu - \mu_0 \cdot \int \frac{H(\mu)}{\mu_0+\mu}\, d\mu = \frac{2}{1+\gamma} - \frac{2}{w}\,\frac{H(\mu_0)-1}{H(\mu_0)}$$

Then

$$A_H = \frac{w}{2} H(\mu_0) \int_0^1 \frac{H(\mu)\mu}{\mu_0+\mu}\, d\mu = 1 - \gamma H(\mu_0)$$

Substituting (10) for $H(\mu_0)$ gives (40).

The hemispherical albedo for scatterers with a phase function $P(g) = (1 + b \cos g)$ will now be obtained. This requires the evaluation of an additional integral of the form (neglecting $B(g)$ as before)

$$2\pi \int_0^1 b \cos g\, \frac{\mu}{\mu_0+\mu}\, d\mu$$

which can be done using the relation

$$\cos g = \mu_0\mu + (1-\mu_0^2)(1-\mu^2)^{1/2} \cos \Phi$$

where Φ is the azimuth angle. This leads to

$$A_H = r_0 \frac{1+\gamma}{1+2\mu_0\gamma} + b\,\frac{w\mu_0}{2}\left(\frac{1}{2} - \mu_0 + \mu_0^2 \ln \frac{1+\mu_0}{\mu_0}\right)$$

If in the Chandrasekhar integral equation for $H(\mu)$, $H(\mu')$ is replaced by its average value $2(1+\gamma)^{-1}$ in the integral and expression (10) for $H(\mu)$ is used elsewhere, the approximation $\mu_0 \ln[(1+\mu_0)/\mu_0] \simeq 2\mu_0/(1+2\mu_0)$ is obtained. Inserting this into the above expression for A_H gives

$$A_H = r_0 \frac{1+\gamma}{1+2\mu_0\gamma} + b\,\frac{w}{4}\,\frac{\mu_0}{1+2\mu_0} \tag{41}$$

Note that a surface of isotropic scatterers illuminated at $i = 60°$ will have $A_H = r_0$ (Figure 8). This result was previously shown by *Reichman* [1973].

h. The Bond Albedo A_B

The Bond albedo is the ratio of light scattered in all directions by a spherical planet of radius R to the light incident on it:

$$A_B = \frac{1}{\pi R^2 J} \int_{A_I} \int_{\Omega_U} Y(\mu_0, \mu, g)\, d\Omega\, dA \tag{42}$$

where $d\Omega = 2\pi\, d\mu$, $dA = 2\pi R^2\, dR$, and A_I is the illuminated hemisphere.

Again, some relations derived by *Chandrasekhar* [1960] will be used and the contributions of $B(g)$ to the integral will be neglected, as justified above. The case of isotropic scatterers will be considered first. Following the same procedure as in section 4g, it can readily be shown that the first integral in (42) is

$$\int_{\Omega_U} Y\, d\Omega = \int_0^1 J\,\frac{w}{4\pi}\,\frac{\mu_0\mu}{\mu_0+\mu} H(\mu_0)H(\mu) 2\pi\, d\mu = J\mu_0[1 - \gamma H(\mu_0)]$$

Thus

$$A_B = \frac{1}{\pi R^2 J} \int_0^1 \mu_0 J[1 - \gamma H(\mu_0)] 2\pi R^2\, d\mu_0 = 1 - 2\gamma \int_0^1 \mu H(\mu)\, d\mu \tag{42'}$$

To evaluate the integral in the second term on the right, we note that $H(\mu)$ is very nearly a linear function of μ (Figure 3). Then $H(\mu)$ is replaced by a linear function having the properties that

$$H(0.5) = \langle H \rangle = \frac{2}{1+\gamma}$$

and

$$\frac{dH}{d\mu}(0.5) = \frac{d}{d\mu}\left(\frac{1+2\mu}{1+2\mu\gamma}\right)\Bigg|_{0.5} = \frac{2}{1+\gamma} r_0$$

Thus the linear approximation to the H-function is obtained

$$H(\mu) = \frac{2}{1+\gamma}[1 + r_0(\mu - 0.5)]$$

Putting this approximation for $H(\mu)$ into (42') gives for isotropic scatterers

$$A_B = r_0\left(1 - \frac{1}{3}\,\frac{\gamma}{1+\gamma}\right) \tag{43}$$

Chamberlain and Smith [1970] have tabulated values of A_B using computer evaluation of the integral in (42'). Comparison of values calculated using (43) with Chamberlain and Smith's values shows that the two agree within 1% everywhere, thus justifying the approximations.

To obtain an approximate expression for particles with the phase function $P(g) = (1 + b \cos g)$ the approximation used in reaching (41) will be made again. Then only an integral of the form

$$\int_0^1 b\,\frac{\mu_0^2}{1+2\mu_0}\, d\mu_0$$

must be evaluated. This integral is straightforward and gives

$$A_B = r_0\left[1 - \frac{1}{3}\,\frac{\gamma}{1+\gamma} + b\,\frac{\ln 3}{16}(1+\gamma)^2\right] \tag{43'}$$

Figure 8 shows A_B as a function of w for isotropic scatterers. For low-albedo materials, $\gamma/(1+\gamma) \simeq \frac{1}{2}$; thus a planet covered with dark, isotropic scatterers has $A_B \simeq 5r_0/6$.

i. The Physical or Geometric Albedo A_P

The physical or geometric albedo is the ratio of the brightness of a planet of radius R at zero phase to the brightness of a Lambert disk of the same radius viewed normally at zero phase.

$$A_P = \frac{1}{JR^2} \int_{A_I} Y(\mu_0, \mu_0, 0)\, dA$$

The case of well-separated isotropic scatterers will be considered first. Then

$$A_P = \frac{w}{4} \int_0^1 H^2(\mu)\mu\, d\mu$$

Using the linear approximation for $H(\mu)$ to evaluate this integral and ignoring terms of order $r_0^3/24$ gives

$$A_P = r_0/2 + r_0^2/6$$

Chamberlain and Smith [1970] have calculated A_P numerically using Chandrasekhar's exact solution for isotropic scatterers and no opposition effect. The values calculated using the last expression agree with exact values to better than 3%, again justifying the approximations.

For nonisotropic scatterers of arbitrary phase function with a finite opposition effect, an additional integral of the form

$$\int_0^1 [(1 + B_0)P(0) - 1]\,\mu\,d\mu$$

must be evaluated, which is trivial and gives

$$A_P = \tfrac{1}{2}r_0\,(1 + \tfrac{1}{3}r_0) + \frac{w}{8}[(1 + B_0)P(0) - 1] \qquad (44)$$

For low-albedo surfaces, $r_0 \simeq w/4$ and $B_0 \simeq 1$, so that $A_P \simeq wP(0)/4$.

j. The Integral Phase Function $\phi(g)$

The integral phase function $\phi(g)$ of a body is the relative brightness of the entire planet at phase angle g, normalized to the brightness at $g = 0°$:

$$\phi(g) = \int_{A_{IV}} Y(\mu_0, \mu, g)\,dA \Big/ \int_{A_{IV}} Y(\mu, \mu, 0)\,dA$$

where A_{IV} is the area of the planet which is both illuminated and visible. These integrations can be carried out using the same approximations as above. The following result ignores terms of order $r_0^3/24$, as justified in section 4*i*:

$$\phi(g) = \frac{r_0}{2A_P}\left\{\left[\frac{(1+\gamma)^2}{4}[(1 + B(g))P(g) - 1] + (1 - r_0)\right]\cdot\left[1 - \sin\frac{|g|}{2}\tan\frac{|g|}{2}\ln\cot\frac{|g|}{4}\right] + \tfrac{4}{3}r_0\,\frac{\sin g + (\pi - g)\cos g}{\pi}\right\} \qquad (45)$$

The initial coefficient in (45) is a normalizing factor. The first term inside the braces is the contribution due to single scattering. Comparison with equation 14 of *Hapke* [1963] shows that it has the same form as the integral phase function of the moon. Thus except for minor differences imposed by $P(g)$, all dark bodies should have phase functions similar to the moon. For bright bodies the second term in braces will dominate, except at very large phase angles. This term is the Schonberg function [*Hapke*, 1963], which describes scattering from a sphere with Lambert surface elements. Thus high-albedo planets will scatter light like a Lambert sphere.

k. The Phase Integral q

The phase integral q is the ratio of the Bond albedo to the physical albedo and is related to the integral phase function as follows:

$$q = A_B/A_P = 2\int_0^\pi \phi(g)\sin g\,dg$$

$$= [\text{equation (43')}]/[\text{equation (44)}] \qquad (46)$$

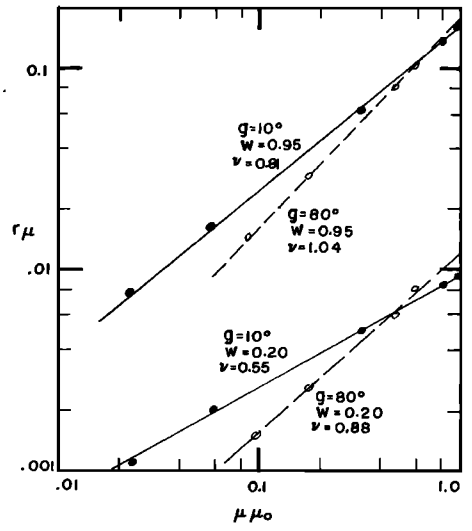

Fig. 9. Minnaert plot of the bidirectional reflectance: log $(r\mu)$ versus log $(\mu_0\mu)$ for several values of the phase angle g and single-scattering albedo w.

In the low-albedo limit, (46) reduces to

$$q \simeq \frac{5}{6}\,\frac{1 + b/3}{1 + b}$$

l. Miscellaneous Topics

The Minnaert function. An empirical function which has been widely used in planetary photometry [e.g., *Thorpe*, 1973] is the Minnaert or generalized Lambert function [*Minnaert*, 1941]

$$\bar{I} = \bar{I}_0\mu_0^{\nu}\mu^{\nu-1}$$

where $\bar{I}$ is the relative brightness of the surface and $\bar{I}_0$ and ν are empirical parameters. To test the validity of the Minnaert function, (16) was used to calculate $(r\mu)$ versus $(\mu_0\mu)$ for a few values of w and g. The results are shown in Figure 9. It is seen that for a given phase angle, $\log(r\mu)$ varies approximately linearly with $\log(\mu_0\mu)$, thus justifying the use of the Minnaert function over limited ranges of angles. However, there are several difficulties with this function. One is that the empirical 'constants' $\bar{I}_0$ and ν are both functions of phase angle. The second is that these parameters are not related in any obvious way to the physical properties of the surface and thus are useless for deducing anything about the surface. *Veverka et al.* [1978] have also pointed out some of the problems with the use of the Minnaert function.

Limb-darkening profiles. The change in brightness as the line of vision approaches the limb or terminator of a body is referred to as the limb-darkening profile. This function can be calculated from (16) for a body with a macroscopically smooth surface. Theoretical limb profiles are compared with spacecraft observations of four planets in paper II. Relative limb-darkening profiles for a macroscopically smooth surface of isotropic scatterers and with $B(g) = 0$ are shown for several values of w in Figure 10. The profiles are strongly dependent on w. The reflectance of a high-albedo planet is dominated by the multiple-scattering term $H(\mu_0)H(\mu)$ and exhibits limb-darkening. A low-albedo planet should exhibit limb-brightening, as required by the mathematical behavior of the Lommel-Seeliger factor $\mu_0/(\mu_0 + \mu)$, which follows rigorously from the solution of the radiative transfer equation.

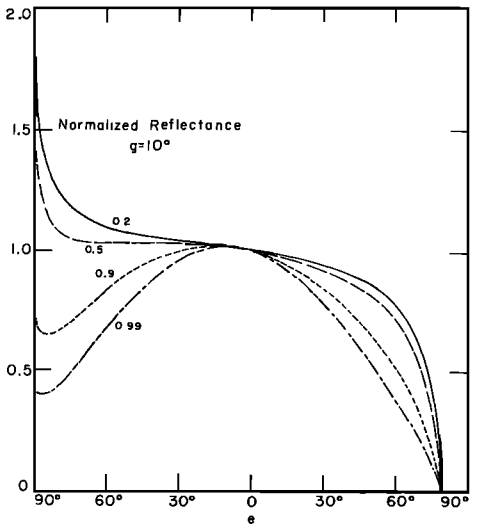

Fig. 10. Planetary limb-darkening profiles: plot of the bidirectional reflectance along the luminance equator, normalized to the sub-observer point, for several values of the single-scattering albedo w.

However, the profile will also be affected by macroscopic surface roughness, especially near the limb. The scale of the roughness must be small compared with the size of the area being examined (typically of the order of several hundred square kilometers) but large compared to the extinction mean free path in the medium, $(\sum_i N_i \sigma_i Q_{Ei})^{-1}$. Near the center of the disk the limb-darkening profiles are relatively flat and local slopes will have little effect. Near the limbs the slopes facing the observer are preferentially visible, while slopes facing away are preferentially blocked. Thus the local apparent limb brightness will take on values appropriate to areas nearer to the center of the disk. Near the terminator the roughness also casts shadows so that the average brighness is not strongly altered. *Hapke* [1966] demonstrated that introducing macroscopic surface roughness into the theoretical lunar photometric function could eliminate the limb-brightening predicted by the Lommel-Seeliger expression.

It is possible to invert this reasoning and use the measured limb-darkening profile to estimate the average macroscopic surface roughness [*Hapke,* 1977] (see also paper II). To do this, there must be sufficient photometric data available that the average single-scattering albedo can be estimated and the theoretical limb-darkening profile calculated. The average macroscopic slope can then be estimated by noting the change in luminance longitude through which a nominally horizontal area at the limb must be tilted to reduce the theoretical brightness to that actually measured. Because of cohesion in a soil, small-scale slopes can be much greater than large-scale slopes and can be influenced by gravity. Thus the average slopes measured by the limb-darkening profile method are primarily those on a small scale (1 mm to 1 m).

Effects of atmospheric hazes. Atmospheric hazes will also modify the limb profile. This effect is especially important for photometry of Mars, where meteorological processes lift surface particles into the atmosphere and keep them suspended for many days and weeks. The vertical density distribution of scattering particles does not appear in (16) explicitly; however, lifting some of the particles into a low-density haze layer will have four indirect effects. First, it will decrease the opposition effect $B(g)$ to zero for those particles which are well-separated, thus decreasing the relative brightness at small phase angles. Second, the haze particles will become forward scatterers due to diffraction becoming important as the average spacing between particles increases. This effect will decrease the brightness at small phase angles but will increase it at large angles. Third, the extinction mean free path increases dramatically from a distance of the order of the mean particle diameter to as much as several kilometers, depending on the haze density, a distance which may be large compared to the undulations on the surface or in the haze layer. For a low-albedo planet this effect will alter the limb-darkening profile in such a way that it will increase the brightness of areas near the sunlit limb. Fourth, if the particles are very small, they will tend to form clumps on the surface. The average single-scattering albedo will effectively be that of the clumps and will be relatively low for absorbing particles. Upon being lifted into the haze the particles may separate and their average albedo increase considerably. Thus creation of a haze may either darken or brighten a surface at small phase angles near the center of the disk, depending on the single-scattering albedo and particle size, but it will nearly always brighten the surface at large phase angles.

Phase effects. The reflectance spectrum of a surface is affected in several ways by the angles at which the surface is viewed and illuminated. First, $P(g)$ depends on the translucency of the particles. As the wavelength increases, many substances, particularly silicates, become less absorbing because of strong absorption bands in the UV [*Wells and Hapke,* 1977] and more radiation is transmitted through the particles. This explains the well-known lunar phenomena of phase-reddening [*Gehrels et al.,* 1964].

Second, the relative contribution of multiply scattered light depends not only on w but also on i and e. As is obvious from (10) and Figure 3, the H-functions are maximum when i and e are near 0°. Consider a substance with strong spectral contrast, so that $w(\lambda)$ in the center of an absorption band is so small that multiple scattering is negligible, but in the wings of the band $w(\lambda) \simeq 1$. The ratio of wing-to-center brightnesses will be much greater when the surface is viewed and illuminated vertically than when viewed and illuminated obliquely. Such effects must always be considered when comparing laboratory and planetary reflectance spectra.

5. CONCLUSIONS

The theory developed in this paper can be used to make quantitative estimates of a number of the properties of the surface or cloud top of a planet, and of absorption coefficients in the laboratory. From the laboratory spectral reflectance of a monomineralic powder the spectrum of the espat-function, $W(\lambda)$ can be calculated, which is approximately equal to twice the absorption optical thickness of the particles. If the average particle size is known, the absorption spectrum can be calculated absolutely. This technique of measuring absorption coefficients by reflectance of powders is especially useful for materials with large α, where transmission methods are difficult. The expressions developed in this paper also allow measurements of $\alpha(\lambda)$ or $r(\lambda)$ of various substances made in the laboratory to be corrected to planetary conditions to take account of different lighting and viewing angles and particle sizes.

If the absolute reflectance of a planet can be measured at only one phase angle, w can be estimated by assuming the surface scatters are isotropic. Further measurements of reflectances at several phase angles gives the average single-particle phase function $P(g)$ and a better measurement of w. For large,

closely spaced, nonopaque particles w is the average of $(1 + \alpha D_e)^{-1}$ weighted by total area of each particle type. If further information is available, such as knowledge of the mean particle size and mineralogy, the components of w may be deconvolved, and quantitative estimates of mineral or elemental abundances made. From the presence or absence of an opposition effect it may be determined whether the particles are far apart, as in a cloud or haze, or closely packed, as in soil. Finally, comparison of observed and theoretical limb-darkening profiles allows an estimate of the mean macroscopic slope to be made.

6. NOTATION

A_B Bond albedo.
A_H hemispherical albedo (directional-hemispherical reflectance).
A_P physical or geometric albedo.
da sensitive area of detector.
$B(g)$ backscatter function which describes the opposition effect.
b, c coefficients in the Legendre polynomial expansion of $P(g)$.
D particle diameter.
D_e effective particle size.
E average extinction coefficient of the medium, equal to $K + S$.
e angle of emergence.
F_D average hemispherically integrated radiance traveling in the downward direction.
F_U average hemispherically integrated radiance traveling in the upward direction.
$f'(\theta), f''(\theta)$ Fresnel reflection coefficients.
g phase angle.
$G(\Omega', \Omega)$ differential scattering coefficient.
$H(\mu)$ function appearing in the reflectance equation.
h parameter determined by surface porosity appearing in $B(g)$.
I radiance or specific intensity.
$\bar{I}(\mu_0, \mu, g)$ reflected radiance from surface at detector, or absolute surface brightness.
i angle of incidence; also subscript denoting the ith type of particle.
J projected irradiance or illuminance, intensity of collimated incident light, insolation.
$j = (-1)^{1/2}$.
K average absorption coefficient of the medium.
k ratio of the imaginary part of the index of refraction to the real part.
L mean spacing between particles $= N^{-1/3}$.
M bulk density, equal to average mass per unit volume.
m complex index of refraction, equal to $n(1 - jk)$.
N number of particles per unit volume.
n real part of index of refraction.
$P(g)$ average phase function of particles.
$p_i(g)$ phase function of ith type of particle.
Q_A absorption efficiency.
Q_E extinction efficiency.
Q_S scattering efficiency.
q phase integral.
R distance to detector; also radius of planet.
$r(\mu_0, \mu, g)$ bidirectional reflectance.
r_C radiance coefficient.
r_F radiance factor.
r_L reflectance of a Lambert surface.
r_o bihemispherical reflectance for isotropic scatterers (Kubelka-Munk equation).
S average scattering coefficient of the medium.
S_E surface scattering coefficient of a particle for diffuse light incident externally.
S_I surface scattering coefficient of a particle for diffuse light incident internally.
s volume scattering coefficient inside particle.
ds element of length.
u extinction optical thickness, equal to $\int_0^z E\, dz$.
W espat-function.
w average single-scattering albedo.
X size parameter, equal to $\pi D/\lambda$.
Y luminance, equal to power radiated per unit area of surface into unit solid angle.
y radius of circle having same projected area as the average opening between particles.
z vertical dimension (positive upward).
α volume absorption coefficient inside particle.
$\gamma = (1 - w)^{1/2}$.
θ angle between ds and z.
λ wavelength.
μ cos e.
μ_0 cos i.
ρ solid density of particle.
σ geometrical cross-sectional area of particle.
ϕ azimuth angle measured from plane of normal to surface and direction into which incident light is moving.
ϕ integral phase function.
Ω direction radiation is moving.
Ω_D direction to detector from surface.
Ω_0 direction to source from surface.
$d\omega$ solid angle from which detector is sensitive to radiation.
$d\Omega_D$ solid angle into which surface emits radiation.

Acknowledgments. I thank E. Wells and R. Nelson and especially C. Rangel for contributions to this work. This research is supported by grants from the National Aeronautics and Space Administration Planetary Geology Program.

REFERENCES

Blevin, W., and W. Brown, Effect of particle separation on the reflectance of semi-infinite diffusers, *J. Opt. Soc. Am., 57*, 129–134, 1967.
Chamberlain, J., and G. Smith, Interpretation of the Venus CO_2 absorption bands, *Astrophys. J., 160*, 755–765, 1970.
Chandrasekhar, S., *Radiative Transfer*, Dover, New York, 1960.
Chylek, P., G. Grams, and R. Pinnick, Light scattering by irregular, randomly oriented particles, *Science, 193*, 480–482, 1976.
Deirmendjian, D., *Electromagnetic Scattering on Spherical Dispersions*. Elsevier, New York, 1969.
Egan, W., and T. Hilgeman, Retroreflectance measurements of photometric standards and coatings, *Appl. Opt., 15*, 1845–1849, 1976.
Esposito, L., Extensions to the classical calculation of the effect of mutual shadowing in diffuse reflection, *Icarus, 39*, 69–80, 1979.
Gehrels, T., T. Coffen, and D. Owings, Wavelength dependence of polarization, III, The lunar surface, *Astron. J., 69*, 826–852, 1964.
Giese, R., and R. Zerull, Zodiacal light models based on nonspherical particles, in *Planets, Stars and Nebulae Studied With Photopolarimetry*, edited by T. Gehrels, pp. 804–813, University of Arizona Press, Tucson, 1974.
Hansen, J., and L. Travis, Light scattering in planetary atmospheres, *Space Sci. Rev., 16*, 527–610, 1974.
Hapke, B., A theoretical photometric function for the lunar surface, *J. Geophys. Res., 68*, 4571–4586, 1963.
Hapke, B., An improved lunar theoretical photometric function, *Astron. J., 71*, 333–339, 1966.

Hapke, B., On the particle size distribution of lunar soil, *Planet. Space Sci., 16*, 101–110, 1968.

Hapke, B., Interpretations of optical observations of Mercury and the moon, *Phys. Earth Planet. Inter., 15*, 264–274, 1977.

Hapke, B., and E. Wells, Bidirectional reflectance spectroscopy, II, Experiments and observations, *J. Geophys. Res.*, this issue.

Hodkinson, J., Light Scattering and extinction by irregular particles larger than the wavelength, in *Electromagnetic Scattering*, edited by M. Kerker, pp. 87–100, Macmillan, New York, 1963.

Hodkinson, J., and I. Greenleaves, Computations of light scattering and extinction by spheres according to diffraction and geometrical optics, and some comparisons with the Mie theory, *J. Opt. Soc. Am., 53*, 577–588, 1963.

Irvine, W., The shadowing effect in diffuse reflection, *J. Geophys. Res., 71*, 2931–2938, 1966.

Irvine, W., Multiple scattering in planetary atmospheres, *Icarus, 25*, 175–204, 1975.

Judd, D., Terms, definitions and symbols in reflectometry, *J. Opt. Soc. Am., 57*, 445–452, 1967.

Kerker, M., *The Scattering of Light and Other Electromagnetic Radiation*, Academic, New York, 1969.

Kortum, G., *Reflectance Spectroscopy*, Springer, New York, 1969.

Kottler, F., The elements of radiative transfer, in *Progress in Optics*, vol. III, edited by E. Wolf, pp. 3–28, North-Holland, Amsterdam, 1964.

Kubelka, P., New contribution to the optics of intensely light scattering materials, I, *J. Opt. Soc. Am., 38*, 448–457, 1948.

Lumme, K., Interpretation of the light curves of some non-atmospheric bodies in the solar system, *Astrophys. Space Sci., 13*, 219–230, 1971.

Meador, W., and W. Weaver, A photometric function for diffuse reflection by particulate materials, *NASA Tech. Note, TN D-7903*, 1975.

Melamed, N., Optical properties of powders, I, Optical absorption coefficients and the absolute value of the diffuse reflectance, II, Properties of luminescent powders, *J. Appl. Phys., 34*, 560–570, 1963.

Minnaert, M., The reciprocity principle in lunar photometry, *Astrophys. J., 93*, 403–410, 1941.

Ney, E., and K. Merrill, Comet West and the scattering function of cometary dust, *Science, 194*, 1051–1053, 1976.

Nicodemus, F., Directional reflectance and emissivity of an opaque surface, *Appl. Opt., 4*, 767–773, 1965.

O'Leary, B., and L. Jackel, The 1969 opposition effect of Mars full disk, Syrtis Major and Arabis, *Icarus, 13*, 437–448, 1970.

Price, M., Optical scattering properties of Saturn's ring, II, *Icarus, 23*, 388–398, 1974.

Reichman, J., Determination of absorption and scattering coefficients for nonhomogeneous media. I, Theory, *Appl. Opt., 12*, 1811–1823, 1973.

Thorpe, T., Mariner 9 photometric observations of Mars from November 1971 through March 1972, *Icarus, 20*, 482–489, 1973.

Van de Hulst, H., *Light Scattering by Small Particles*, John Wiley, New York, 1957.

Van de Hulst, H., A new look at multiple scattering, technical report, Goddard Inst. for Space Stud., New York, 1963.

Veverka, J., Photometry and polarimetry, in *The Atmosphere of Titan*, edited by D. Hunten, *NASA Spec. Publ., SP-340*, 42–57, 1974.

Veverka, J., J. Goguen, S. Yang, and J. Elliot, Scattering of light from particulate surfaces, I, A laboratory assessment of multiple scattering effects, *Icarus, 34*, 406–414, 1978.

Wells, E., and B. Hapke, Lunar soil: Iron and titanium bands in the glass fraction, *Science, 195*, 977–979, 1977.

Wendtland, M., and H. Hecht, *Reflectance Spectroscopy*, John Wiley, New York, 1966.

Zerull, R., Scattering functions of dielectric and absorbing irregular particles, in *Interplanetary Dust and Zodiacal light*, edited by H. Elsasser and H. Fechtig, pp. 130–134, Springer, New York, 1976.

Zerull, R., and R. Giese, Microwave analogue studies, in *Planets, Stars and Nebula Studied by Photopolarimetry*, edited by T. Gehrels, pp. 901–915, University of Arizona Press, Tucson, 1974.

Zerull, R., R. Giese, and K. Weiss, Scattering functions of non-spherical dielectric and absorbing particles vs. Mie theory, *Appl. Opt., 16*, 777–778, 1977.

(Received April 24, 1978;
revised October 13, 1980;
accepted October 23, 1980.)